minerals

IMPACT FACTOR 2.2

CITESCORE 4.1

Article

The Role of Mineral and Organic Composition on the Phosphorus Content of Prehistoric Pottery (Middle Neolithic to Late Bronze Age) from NW Spain

María Guadalupe Castro González, María Pilar Prieto Martínez and Antonio Martínez Cortizas

Special Issue
The Significance of Applied Mineralogy in Archaeometry

Edited by
Dr. Stefano Pagnotta and Prof. Dr. Marco Lezzerini

MDPI

https://doi.org/10.3390/min14090880

minerals

MDPI

Article

The Role of Mineral and Organic Composition on the Phosphorus Content of Prehistoric Pottery (Middle Neolithic to Late Bronze Age) from NW Spain

María Guadalupe Castro González [1,2], María Pilar Prieto Martínez [1,2] and Antonio Martínez Cortizas [3,4,*]

[1] Centro de Investigación Interuniversitario de los Paisajes Atlánticos Culturales (CISPAC), Edificio Fontán, Cidade da Cultura, 15707 Santiago de Compostela, Spain; guadalupe.castro@usc.es (M.G.C.G.); pilar.prieto@usc.es (M.P.P.M.)
[2] EcoPast, Facultade de Xeografía e Historia, Universidade de Santiago de Compostela, 15782 Santiago de Compostela, Spain
[3] Centro de Investigación Interdisciplinar en Tecnoloxías Ambientais (CRETUS), EcoPast, Facultade de Bioloxía, Universidade de Santiago de Compostela, Campus Vida, Rúa de Lope Gómez de Marzoa, 15, 15782 Santiago de Compostela, Spain
[4] Bolin Centre for Climate Research, Stockholm University, 10691 Stockholm, Sweden
* Correspondence: antonio.martinez.cortizas@usc.es

Abstract: Phosphorus is a key element for identifying past human activity. Recently, phosphorus analyses have been extended to archaeological objects, aiming at distinguishing how depositional contexts contribute to its enrichment. In archaeological pottery, phosphorus might depend on several manufacturing and postdepositional processes (i.e., addition of organic temper, pigments, diagenetic incorporation). We analyzed by XRD, XRF, and mid-infrared (FTIR-ATR) spectroscopy 178 pots from eight NW Spain archaeological sites. These sites encompass different chronologies, contexts, and local geology. The phosphorus content was highly variable (224–27,722 mg kg^{-1}) overall but also between archeological sites (1644 ± 487 to 13,635 ± 6623 mg kg^{-1}) and within archaeological sites (4–36, max/min ratio). No phosphate minerals were identified by XRD nor FTIR-ATR, but correlations between phosphorus content and MIR absorbances showed maxima at 1515 and 980 cm^{-1}, suggesting the presence of two sources: one organic (i.e., phosphorylated aromatic compounds) and another inorganic (i.e., albite and K-feldspar). Phosphorylated aromatics were most likely formed during pottery firing and were preserved due to their high resistance to temperature and oxidation. Meanwhile, albite and K-feldspar are among the P-bearing minerals with higher P concentrations. Our results suggest that P content is related to intentional and non-intentional actions taken in the pottery production process.

Keywords: phosphorus; prehistoric pottery; NW Spain; XRF; XRD; FTIR-ATR; albite; K-feldspar; aromatics phosphorylation

Citation: Castro González, M.G.; Prieto Martínez, M.P.; Martínez Cortizas, A. The Role of Mineral and Organic Composition on the Phosphorus Content of Prehistoric Pottery (Middle Neolithic to Late Bronze Age) from NW Spain. *Minerals* **2024**, *14*, 880. https://doi.org/10.3390/min14090880

Academic Editor: Domenico Miriello

Received: 31 July 2024
Revised: 20 August 2024
Accepted: 25 August 2024
Published: 29 August 2024

1. Introduction

Phosphorus is a fundamental chemical element in archaeology that can be used to identify past human activity in soils [1–5]. Extensive research has shown that inorganic and organic phosphorus can be used as a proxy to distinguish among several human activities. For example, associations have been established between different phosphorus-rich soils and archaeological and ethnological contexts such as hearths, middens, food preparation areas, butchering spaces and ceremonial areas with organic offerings [3,6,7] or to prove the existence of necropolises in areas with no or poor bone preservation [8–14].

This diverse range of geochemical studies in archaeology involves using soil as a repository for traces of past human activity or vanished remains. In other words, these studies use signals of diagenesis in soils to identify activities from the past. However, diagenesis in the context of material culture is traditionally concerned with the preservation of artifacts

and ecofacts rather than using diagenetic signals as indicators of human activity [15]. This is particularly evident in the case of materials such as metals [16,17] or bone [18–20].

With this research background, pottery has a rich tradition of studies that focus on its mineralogical, chemical, and structural changes resulting from production and post-depositional processes [21–24], and some of them exclusively analyzed how diagenetic processes can affect the original compositional signature of pottery [25–29]. Moreover, new approaches in pottery diagenesis studies have noted that post-depositional changes in vessels, many of which are associated with the formation of secondary phosphates, could potentially contribute to the characterization of the pottery's deposition context as a collateral result [30–32]. Additionally, phosphorus in pottery has not only been interpreted as part of a diagenetic processes but also as an indicator of its production processes. In both archaeological and ethnoarchaeological literature, several phosphorus-enriched materials, like bone, ash or dung, have been mentioned as temper or incrustations in ceramic decorations [33–39]. Another possibility is the enrichment of phosphorus in pottery vessels due to their use as cooking pots [40] or the use of pigments [41].

Our study aims to enhance the understanding of the phosphorus enrichment in ancient pottery by exploring the three previous outlined key hypotheses. First, the enrichment in phosphorus results from diagenetic processes, which might be linked to specific past human activities and geochemical conditions of the soils where the pots were buried. Second, the presence of phosphorus in ancient pottery was a consequence of intentional and unintentional actions in the pottery production process. And third, the incorporation of phosphorus was a result of the use of the pots (i.e., cooking food). To achieve these objectives, we analyzed by XRD, XRF, and FTIR-ATR, 178 sherds from prehistoric pottery recovered in eight archaeological sites that represent a large time span (mid-Neolithic to late Bronze Age), various depositional contexts (settlements, middens, funerary areas, etc.), and located in areas with contrasting lithologies which may have influenced the available raw materials and geological P content.

2. Materials and Methods

2.1. Sample Assemblage

Sherds (178) from eight prehistoric sites from Galicia (NW of Spain) were selected for this study. The sites encompass different functional areas, including funerary monuments, flat graves, gathering areas, hearths, middens, and domestic spaces (Figure 1). Chronologically, the sample includes pottery from the Middle Neolithic to the Late Bronze Age (4600/4000–800/700 BC). The local lithology of the areas where the sites are located was also considered, as it is known that rocks with granitic compositions (i.e., felsic) are richer in P than basic and ultrabasic (i.e., mafic) rocks [42]. Thus, we aimed to achieve a similar representation across chronologies, contexts, and geochemical compositions. Additionally, other pottery manufacturing features, such as temper, and the level of mineral inclusions, and firing atmosphere, are also provided in the supporting material. These properties were correlated to phosphorus content (as well as C and N), and we found no significant effect or correlation. Thus, they are not further discussed.

In terms of statistical coherence, these sherds constitute a large set with various potential determining factors, as chronologies, depositional context, etc. (see Supplementary Materials S1 and Supplementary References for further information about the archaeological context and selection of the samples).

Samples were prepared by thoroughly cleaning the sherds with water to remove any possible sediment remains. After cleaning, a fragment of each sherd was ground in a Retsch MM301 (Retsch GmbH, Haan, Germany) mill to achieve a fine powder (<50 μm) before analysis.

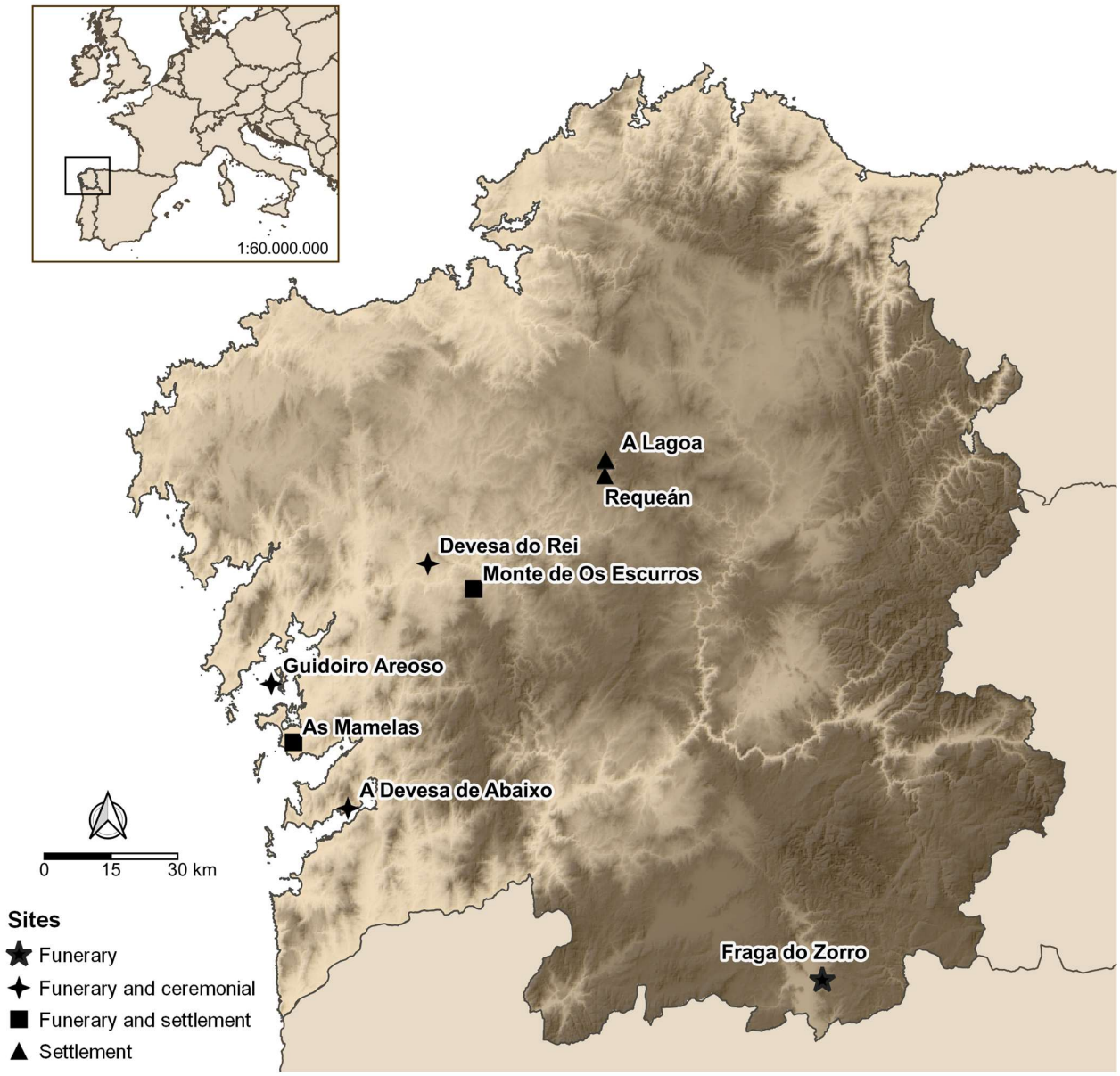

Figure 1. Location of the selected sites in Galicia (NW Spain). The symbols represent the functional features of each site. Base maps: CNIG—https://centrodedescargas.cnig.es/CentroDescargas/busquedaSerie.do?codSerie=02102-BTN25 (accessed on 17 May 2024) and Eurostat/GISCO—https://ec.europa.eu/eurostat/web/gisco/geodata/administrative-units/countries (accessed on 04/06/2024). Figure created using QGIS 3.28.12. QGIS.org, 2023. QGIS Geographic Information System. QGIS Association. http://www.qgis.org (accessed on 24 August 2024).

2.2. Mineralogical Analysis (XRD)

All sherds were analyzed by X-ray diffraction to characterize their mineralogical composition. A Philips PW1710 diffractometer equipped with a Bragg–Brentano θ/2θ vertical goniometer and a 2.2 Kw generator with Cu anode, graphite monochromator and a PW1711/10 proportional detector was used (Malvern Panalytical, Malvern, Worcestershire, UK). The equipment is hosted at the XRD facility of the Infrastructure Network for the Support of Research and Technological Development of Universidade de Santiago de Compostela (RIAIDT-USC). For mineral identification and quantification, DIFRACplus EVA v 5.1 (Bruker AXS) (Bruker, Billerica, MA, USA) and HighScore Plus (PANanalytical BV 2011) (Malvern Panalytical, Malvern, Worcestershire, UK) software packages were employed.

This facility meets the ISO:2015 standards—https://assets.usc.gal/sites/default/files/paragraphs/more_info_service/2023-06/DNV_Certificate-English_v2023.pdf (accessed 24 August 2024) Semiquantification of mineral abundances was performed using the RIR (reference intensity ratio) method [43] and the HighScore Plus Release v3.0d software of Malvern Panalytical (Malvern Panalytical, Malvern, Worcestershire, UK).

Previous XRD research on smaller sets of ceramics of the studied region [44–46], as well as comparison at a European scale [47], have already provided consistent results.

2.3. Elemental Analysis (XRF and CN Analyzer)

X-ray fluorescence spectrometry (XRF) was used to quantify the elemental composition of pottery. Depending on the chemical element, different primary and secondary anodes were used: a primary silver anode and a secondary pyrolytic graphite anode (for Al, Si, P, and S), a primary silver anode and a secondary iron anode (for K, Ca), and a primary molybdenum anode (for Fe, Rb, and Sr). The equipment was calibrated using certified reference materials (NIST 198, 278, 607, 679, 688, 694, 1400, 1413, 1486, 1646, 1944, 2586, 2690, 2691, 2702, 2703, 2780, 5365, 8704, 1646a, 1d, 2709a, 277b, 634a, 640b, 70a, 78a, 81a, 88b, 97b, 98b, 99b), and for verification, the NIST 97b standard is used. We used the following quantification limits: Si 1000 mg kg^{-1}, Al and K 500 mg kg^{-1}, Ca 200 mg kg^{-1}, P, S and Fe 100 mg kg^{-1}, Sr 5 mg kg^{-1}, Rb 1 mg kg^{-1}. Replicates of the standard reference materials and of selected pottery samples agreed within 10%.

Total carbon and nitrogen contents were measured with a Leco-TruSpec CHNS Elemental Macro Sample Analyzer (LECO Corporation, St. Joseph, MI, USA). Precision was 25 mg kg^{-1} for C (0.5% RSD) and 40 mg kg^{-1} for N (0.5% RSD). The XRF and CHNS equipment were also hosted at RIADIT-USC.

2.4. FTIR-ATR

Mid-infrared (4000–400 cm^{-1}) vibrational spectroscopy was conducted on the finely milled and homogenized samples, using an Agilent Technologies Cary 630 FTIR-ATR (EcoPast laboratory, Universidade de Santiago de Compostela). We used a resolution of 4 cm^{-1} and performed 100 scans per sample. The equipment was thoroughly cleaned, and a background was collected before analyzing each sample. Spectra were processed with the Spectroscopy add-on widgets of the Orange data mining software v3.37.0 [48].

2.5. Statistical Analyses

Principal components analysis (PCA) was applied to the elemental data (XRF and CN analyzer) to extract the main geochemical signals/associations. Before statistical analysis, the elemental concentrations were log-transformed to avoid the close data effect of compositional data. PCA was performed on varimax rotation and on the correlation matrix, using IBM SPSS v29.0.2. To determine the influence of the MIR bands on P and the PCA chemical associations related to P (see below), we followed two approaches: (i) computing the correlation spectrum (i.e., the correlation of the absorbance of each wavenumber of the collected spectra to the target variable) with P concentrations and the PCA components; (ii) applying the FreeViz widget of the software Orange. v3.37.0. FreeViz enables visualizing the distribution of a target variable (as P concentration) as a color map and, at the same time, the distribution of the potential contributors to the target as vectors—the length and direction of the vectors indicating the weight and effect (increase or decrease in the target variable) of the potential contributor. In our case, we used P concentrations and the PCA component accounting for P distribution in the sherds as target variables and selected MIR absorbances (based on the correlation spectra) as potential contributors.

We also used multilinear regression to model P sherds' content. The weights of the predictors (compounds/minerals) were obtained by multiplying the regression coefficient of the predictor by the predictor's value in each sherd. In this way, the P content is decomposed into contributions from each predictor and plotted as a graph of cumulative bars.

3. Results and Discursion

3.1. Mineralogical Composition (XRD)

Eleven minerals belonging to the silicates (10) and oxides/hydroxides (1) classes were identified by XRD in the set of sherds analyzed (Figure 2 and Table S1). Of the silicates, most of them are primary minerals and only one is a secondary mineral (kaolinite); in order of frequency (number of sherds in which the mineral is present) in the set of samples, quartz, plagioclase, and K-feldspars were the most frequent (>80% of the sherds), followed by mica (69%), amphibole (34%), and chlorite (22%); last, kaolinite (10%), talc (8%), epidote (8%), and serpentine (4%) were occasional. Iron oxides (9%) were also occasionally detected.

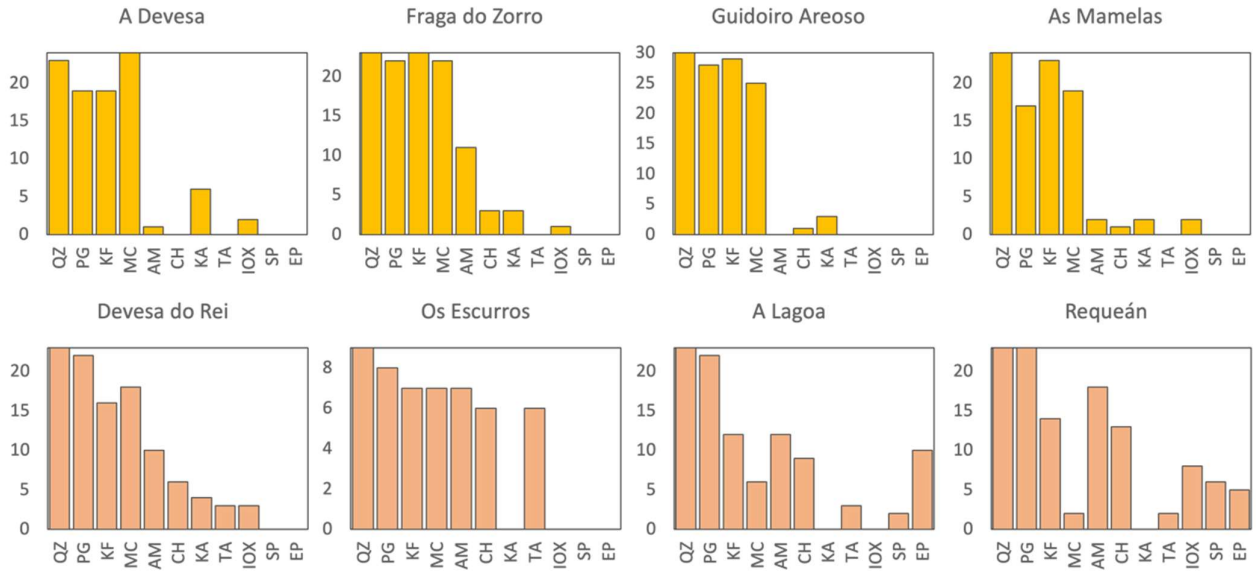

Figure 2. Mineralogy of the studied sherds (number of sherds samples of each site in which the mineral was present). QZ: quartz; PG: plagioclase; KF: K feldspar; MC: micas; AM: amphibole; CH: chlorite; KA: kaolinite; TA: talc; IOX: iron oxides; SP: serpentine; EP: epidote. Yellow: sites on areas of felsic lithologies; orange: sites on areas of mafic lithologies.

Mineralogical differences between sites located in areas of felsic or mafic lithologies are also observed, except for quartz. Plagioclase is slightly more frequent in sherds from sites of mafic areas (96%) than in sherds from sites of felsic areas (85%); K-feldspars (93% vs. 63%), mica (89% vs. 42%), and kaolinite (14% vs. 5%) are more frequent in the latter than in the former. Amphibole (60% vs. 34%) and chlorite (44% vs. 22%) are more frequent in sherds from sites of mafic areas than in those of sites of felsic areas. Talc, serpentine, and epidote were only found in sherds from sites of mafic areas. Iron oxides were detected in both areas but were twice as frequent in sherds from sites of mafic areas. Despite the limitations of the RIR quantification method, the data reflect high variability in terms of abundance of each mineral in the sherds of each archaeological site (Table S1) and thus a quite varied mineralogical composition.

In agreement with previous investigations, no primary P mineral phases were found in the sherds [30,40,49,50]. These phases have been rarely identified in archaeological sherds, being dominantly of the variscite type when found [40].

3.2. Elemental Composition (XRF)

Phosphorus concentrations varied by two orders of magnitude (maximum 27,722 and minimum 224 mg kg^{-1}), showing a large variability between sites (Figure 3; Table S2). Guidoiro Areoso sherds showed the largest average P concentrations (13,635 ± 6623 mg kg^{-1}), which were followed by Fraga do Zorro (8988 ± 3661 mg kg^{-1}), A Lagoa (3967 ± 1578 mg kg^{-1}), Requeán (2963 ± 915 mg kg^{-1}), and Os Escurros (2640 ± 1329 mg kg^{-1}). The lowest

concentrations were found for As Mamelas (1829 ± 971 mg kg^{-1}), A Devesa de Abaixo (1752 ± 1725 mg kg^{-1}), and Devesa do Rei (1647 ± 487 mg kg^{-1}). Moderate variability in concentrations (coefficient of variation, CV 30–50) was shown by all sites, but A Devesa do Rei showed large (CV 98) variability despite the overall lower concentrations.

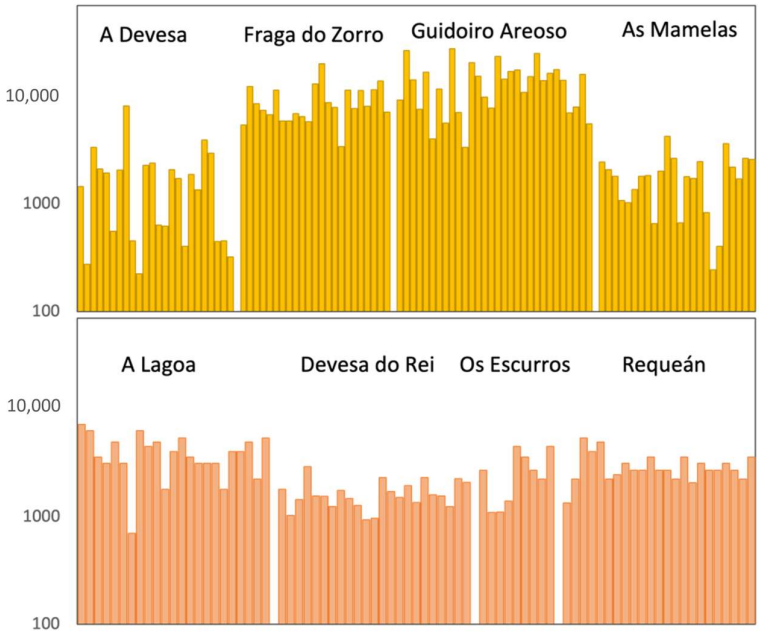

Figure 3. Phosphorus concentration (log scale) of the studied sherds (mg kg^{-1}). Upper panel, sites on areas dominated by felsic geological materials; lower panel, sites from areas dominated by mafic materials.

These P contents, expressed as oxide (P_2O_5), varied between a minimum of 0.05% and a maximum of 6.24%; these values are within the usual range observed in archaeological pottery (0.02%–3.00%) [49,51–56] but well below the 8%–11% obtained by Freestone et al. [57] in prehistoric ceramics from Britain, >10% in Neolithic pottery from Italy [58], and the maximum (9.75%) found by Costa et al. [59] in ceramics from the Amazonian Dark Earth (ADE) soils.

Average concentrations for the other elements determined (C, N, S, Si, Al, Fe, Ca, K, Rb, and Sr) can be found in Table S2. We performed a PCA using all elements and obtained three main components that accounted for 70% of the variance of the geochemical composition of the sherds. The first component, G-Cp1, accounted for 30% of the total variance and showed large positive loadings for Rb, K, and Al and negative loadings for Fe and Ca (Figure 4; Table S3). This component reflects the imprint of the two background lithologies in the analyzed samples: felsic and mafic. As shown in Figures 4 and 5, almost all sherds from sites of areas with dominant felsic lithologies have positive scores (i.e., are relatively enriched in Al, K, and Rb), while sherds from sites of areas with dominant mafic lithologies have negative scores (i.e., are relatively enriched in Fe and Ca). Despite this, all sites, except for Guidoiro Areoso, contained sherds with mafic composition in felsic areas or with felsic composition in mafic areas (Figure 5).

The second component, G-Cp2, accounted for 22% of the total variance and showed large positive loadings for P, Ca and Sr (Figure 4; Table S3). As expected, the scores of this component correlated well with P concentrations (r 0.86) and thus reflect the P variation in the set of sherds analyzed. Overall consistent, positive scores (i.e., relatively high P, Ca, and Sr concentrations) were obtained for Guidoiro Areoso and Requeán (although lower). Consistent, negative scores were found for A Devesa de Abaixo, As Mamelas, Devesa do Rei, and Os Escurros (Figure 5). Fraga do Zorro and A Lagoa showed sherds with positive and negative scores.

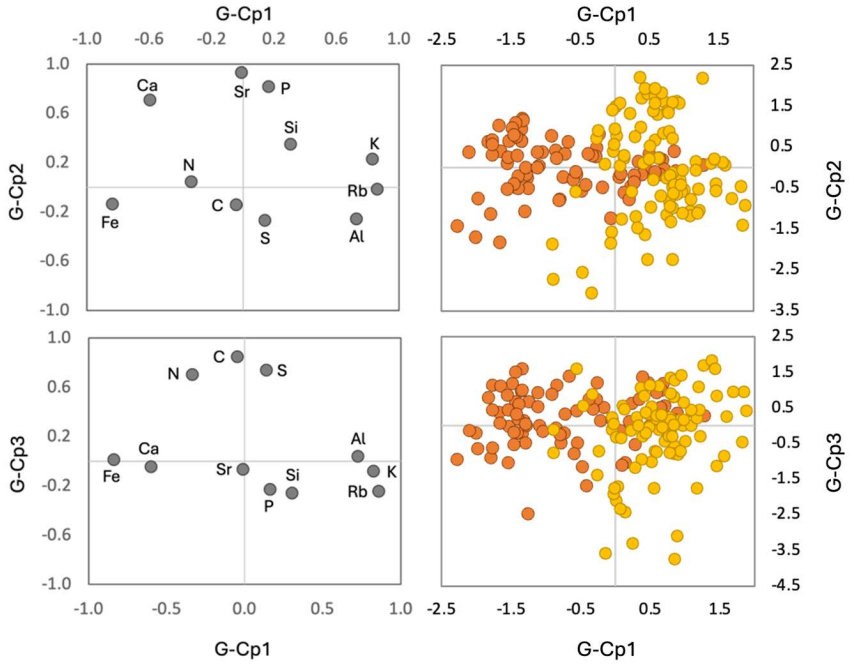

Figure 4. Projections of the loadings of chemical elements (**left**) and the scores of the samples (**right**). Yellow: pots from archaeological sites on areas of felsic lithologies; orange: pots from sites on areas of mafic lithologies.

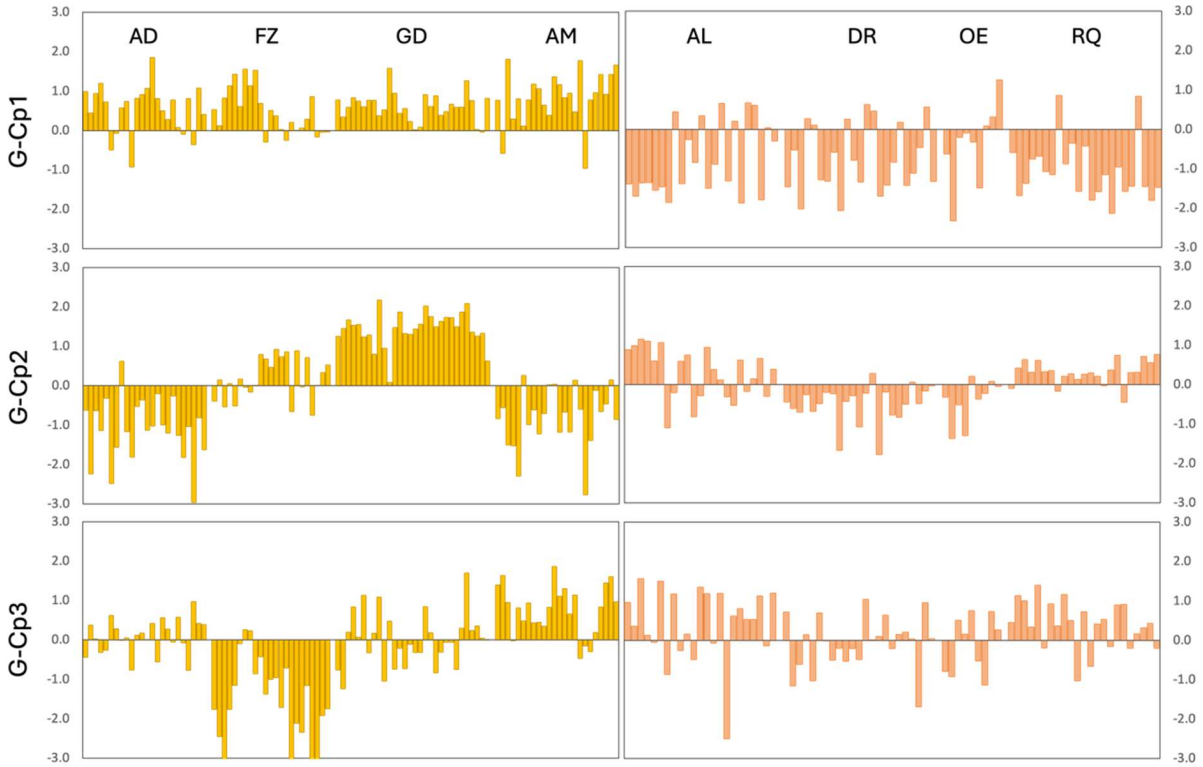

Figure 5. Scores of the analyzed sherds for the three extracted components. Left, sites on areas dominated by felsic geologic materials; right, sites from areas dominated by mafic materials. Sites: AD, A Devesa de Abaixo; FZ, Fraga do Zorro; GD: Guidoiro Areoso; AM: AS Mamelas; AL: A Lagoa; DR: Devesa do Rei; OE: Os Escurros; RQ: Requeán. Yellow: sites on areas of felsic lithologies; orange: sites on areas of mafic lithologies.

The third component, G-Cp3, accounted for 18% of the total variance and showed large positive loadings for C, N, and S (Figure 4; Table S3). Thus, it is related to the organic matter content of the sherds. The distribution of the scores is quite heterogeneous, indicating relatively large variations in organic matter content for each site (Figure 5). The main exceptions are Fraga do Zorro, with large negative scores (i.e., very low total organic matter content), and As Mamelas, which showed positive scores for almost all sherds. The other sites have both sherds with positive (predominant in A Lagoa and Requeán) and negative scores.

It is interesting to note here that the element of interest in this research (P) shows no shared variance with the total content of organic matter nor with the felsic–mafic component. The P–Ca–Sr association of G-Cp2 points to a Ca–phosphate phase but, as indicated above, no P-mineral phases were identified. Some investigations suggested that P, whether sourced from the soil solution [57] or from cooking food [40], precipitates in and around the pores of the ceramics, sometimes as amorphous Al phosphates with a P/Al ratio close to that of the theoretical value for variscite [40]. Phosphorus has a great affinity to bind to Al [42], but the P/Al ratios of the sherds analyzed by us (1.5–243.1 mmol/mol) are highly correlated to P (r 0.98) and almost independent of Al (r −0.39), and the high P/Al ratios, as suggested by Rodrigues and Costa [40], can be taken as an indication that Al phosphates are not responsible for most of the P content of the analyzed sherds.

3.3. FTIR-ATR

The spectra of the studied sherds are represented in Figure 6, which are grouped by archaeological site and geological area. The highest absorbances occur in the region 1200–800 cm^{-1}, with maxima at 1020–1010 cm^{-1} (14% of the sherds), 1005–1000 cm^{-1} (31%), 1000–990 cm^{-1} (37%), 990–980 cm^{-1} (15%), and 950–960 cm^{-1} (4%). Relatively high absorbances were also found at 526, 462, and 423 cm^{-1} in most samples and at 798, 775, and 667 cm^{-1} in some samples. Low absorbances were also detected at 3300, 1700–1500, and 1387 cm^{-1}. Some sherds also showed weak absorbances at 3694 and 3620 cm^{-1}. Almost all the peaks in absorbance can be attributed to vibrations of the main primary minerals detected by XRD (quartz, K feldspar, plagioclase, amphibole, mica, epidote, talc) but also to secondary minerals, such as kaolinite. The signal of iron oxides is difficult to assess, as their main vibrations overlap with those of silicates (as vibrations at 655–650, 535–525, and 470 cm^{-1}). Since kaolinite is present in some of the sherds and in the weathering products of the geological materials (i.e., raw materials of the ceramics) of the area, it is almost certain that metakaolinite is also present in the analyzed sherds. Kaolinite transforms to metakaolinite when firing temperatures exceed 550 °C. Thermal transformation (i.e., dehydroxylation) produces a broad band between 1300 and 600 cm^{-1} [60].

In agreement with the XRD analyses, the MIR spectra provide no clear evidence of the presence of P-mineral phases despite the PCA on the elemental data suggesting the presence of Ca phosphates. PO_4^{3-} ions have absorbances at 1000–1100, 1040, 1020–1120, 602 and 555, and 600–560 cm^{-1}, while HPO_4^{2-} ions have absorbances at 880 and 875 cm^{-1} [61], and non-apatitic PO_4 also absorbs at 617 cm^{-1} [62]. Most of these vibrations overlap with those of silicates, complicating the identification of P-mineral phases and even, as shown below, no significant correlation to P content in the sherds was found for any of them or, when found, the correlation was negative (617 cm^{-1} r −0.42).

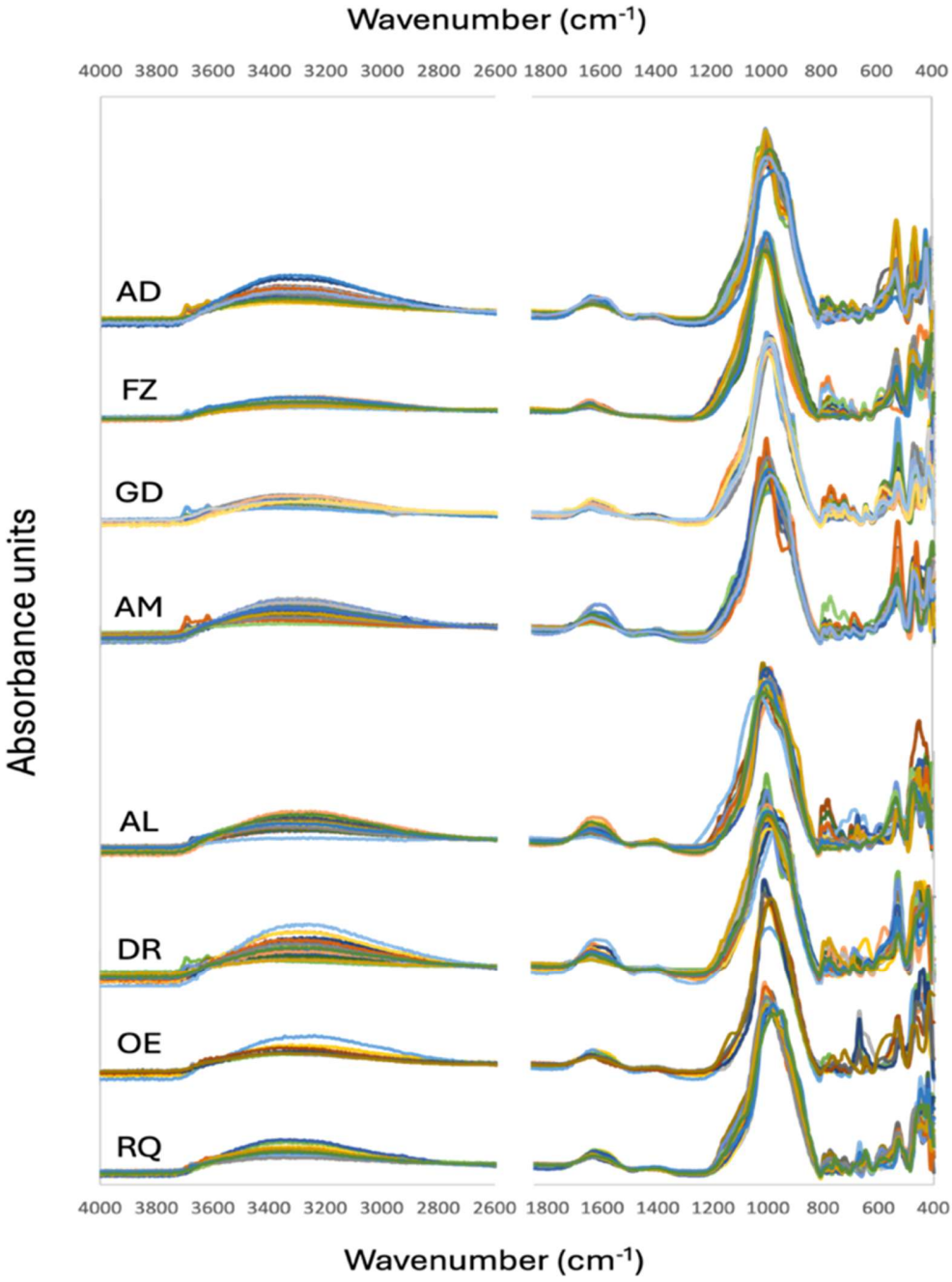

Figure 6. Mid-infrared spectra of the samples analyzed in each archaeological site. Sites: AD: A Devesa de Abaixo; FZ: Fraga do Zorro; GD: Guidoiro Areoso; AM: AS Mamelas; AL: A Lagoa; DR: Devesa do Rei; OE: Os Escurros; RQ: Requeán.

3.4. FTIR-ATR and Phosphorous Content in the Sherds

We will not further discuss the MIR spectral signal in terms of mineralogy as this is the aim of an ongoing research project for a larger collection of sherds from NW Spain. Here, the MIR signal is used to obtain insights into the components related to P (P concentration and G-Cp2 scores) content in the sherds, although additional information is also provided for the other two PCA components extracted on the elemental data (Figure S1).

Figure 7A shows the correlation spectrum for P and G-Cp2, indicating which areas of the MIR signal significantly correlate to both variables. The spectra are almost identical with moderate to low negative correlations in the regions 3700–2700 (peak at 2950 cm^{-1}, $r = -0.46$), 1670–1550 (peak at 1580 cm^{-1}, $r = -0.30$), 950–800 (peak at 915 cm^{-1}, $r = -0.51$),

617 cm^{-1} (r = −0.41), 544 cm^{-1} (r = −0.37), and 468 cm^{-1} (r = −0.36). High positive correlations are found for regions 1530–1490 (peak at 1515 cm^{-1}, r = 0.68), 1450–1420 (peak at 1435 cm^{-1}, r = 0.55), 1360–1120 (peaks at 1357, 1264, and 1146 cm^{-1}, r = 0.44 to 0.46, respectively), 1000–900 cm^{-1} (peak at 980 cm^{-1} r = 0.60), and 760 cm^{-1} (r = 0.38) and 721 cm^{-1} (r = 0.44).

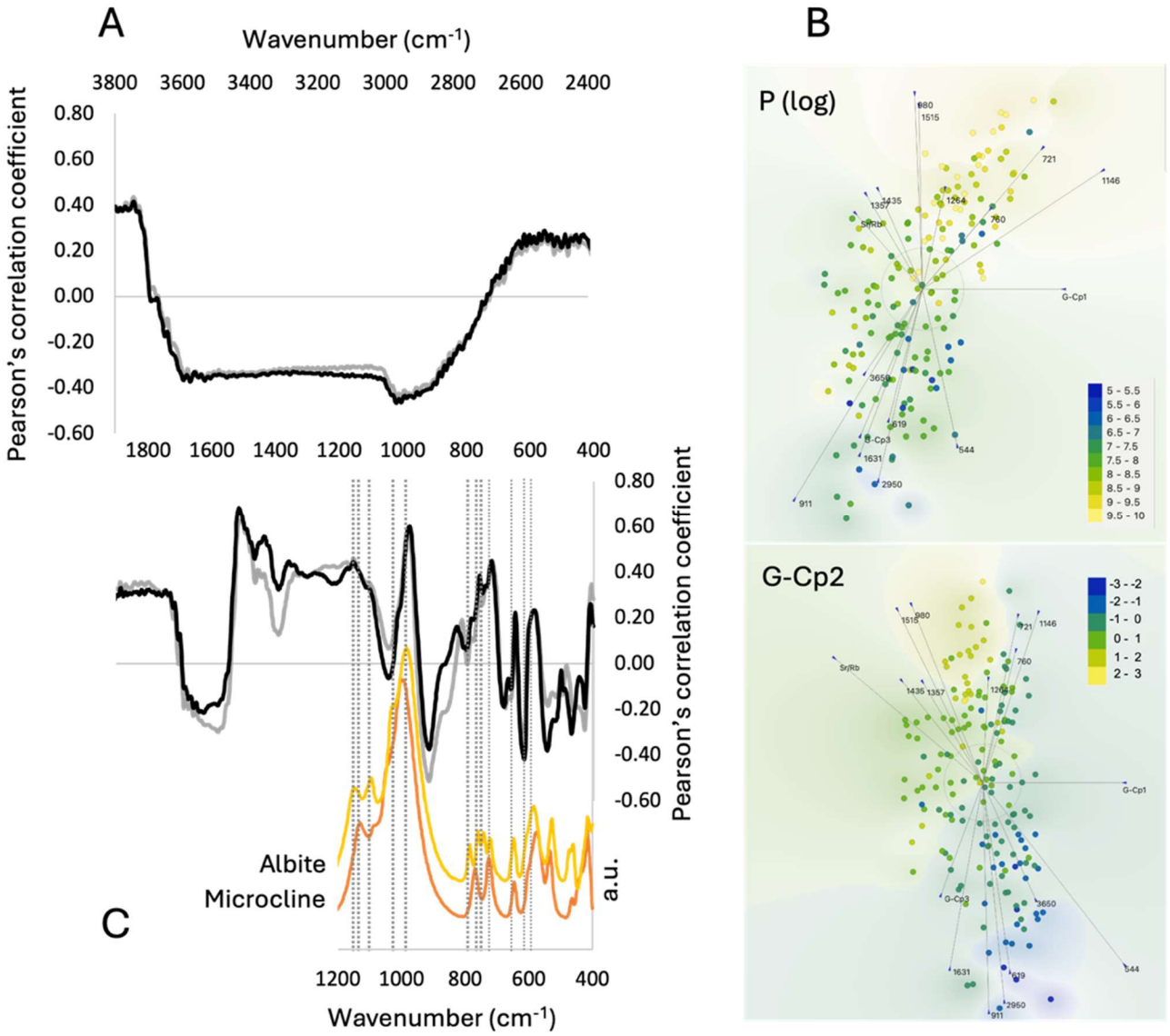

Figure 7. (**A**) Correlation spectra for P (light gray line) and G-Cp2 (black line). (**B**) FreeViz graphs using as target variables P (log)concentrations and G-Cp2 scores, and selected bands of the correlation spectra (normalized absorbances) as influencing variables. (**C**) Spectra of albite and microcline (a.u., absorbance units) obtained from the RRUFF database—https://rruff.info/ (accessed on 24 August 2024).

The FreeViz plot also shows the distribution of the values of the target variables, P and G-Cp2, and the vectors of selected MIR bands of the correlation spectra, which are the other two principal components extracted in the PCA (G-Cp1 and G-Cp3) (Figure 7B). We also included the Sr/Rb ratio as an indicator of the relative abundance of albite vs. K-feldspar (the Sr/Rb ratio is significantly correlated, r = 0.60, with the albite abundance determined by XRD—with the limitations already noted for the XRD semiquantification). Both P and G-Cp2 show a gradient of decreasing values from top to bottom, although the transition

is more clear for G-Cp2. Consequently, the spatial distribution of the vectors is also quite similar. MIR bands associated with high G-Cp2 values (i.e., higher P concentrations) are 980 and 1515 cm^{-1} together with the Sr/Rb ratio and bands at 1435 and 1357 cm^{-1}. A second set, with also high influence, includes bands 1265, 1146, 760, and 721 cm^{-1}. At the other end, of samples with low P concentrations, the largest vectors correspond to MIR bands 911, 2950, 617 and 1631 cm^{-1}, which are followed by 3650 cm^{-1} and G-Cp3. A large vector in this concentration area is also shown by 544 cm^{-1}.

Bands related to sherds with high G-Cp2 scores seem to correspond to mineral phases. The peaks at 980, 1146, 760, and 721 cm^{-1} can correspond to albite and K-feldspar. In fact, the spectra of these two minerals fit with the correlation spectrum of G-Cp2 (and P) for wavenumbers lower than 1200 cm^{-1} (Figure 7C). Albite and K-feldspar are known to be major P hosts in granitic rocks [42,63] and may account for the larger P content in sherds from archaeological sites from felsic (i.e., granitic) areas. They were surely already present in the raw materials and could also have been added as temper to the pots [45,46,64]. Some minerals' vibrations also show large vectors in the region of sherds with low G-Cp2 scores: the bands corresponding to kaolinite (3650, 911, and 544 cm^{-1}). Some investigations have suggested that Al phosphates can form as a result of the collapse of the kaolinite [40,65]. The negative correlation between the peaks of kaolinite in the hydroxyl region (3700–3600 cm^{-1}) and P and G-Cp2, although modest, also supports this hypothesis.

Absorbances on the 1530–1250 cm^{-1} region show large vectors associated with high G-Cp2 scores. These bands correspond to organic compounds and aromatic compounds in particular. Peaks showing the largest correlation to P content (1515, 1435, and 1264 cm^{-1}) are typical of aromatic compounds (i.e., lignin). In a previous investigation on the molecular composition of the organic matter (OM) of archaeological pottery from NW Spain, Kaal et al. [66] found that the OM was dominated by aromatic, pyrogenic compounds, most probably formed upon firing. They also found that the total OM content of the sherds was correlated to aliphatic OM content and not to aromatic OM content. Our data agree with the results of this investigation, as the aromatic signal is dominant in the OM of the sherds we have analyzed, and the total OM of the sherds (i.e., G-Cp3) is positively correlated to the aliphatic vibrations (Figure S1). In the sherds analyzed by us, G-Cp2 and P are positively correlated to the aromatic OM (1550–1200 cm^{-1}) but negatively correlated to aliphatic OM (3000–2800 cm^{-1}) and nitrogenated OM (1631 cm^{-1}) (Figure 7A). G-Cp3, which is related to total OM content (C, N and S), also shows a moderate vector in the region of low G-Cp2 scores (Figure 7A,B)

3.5. Regression Model for Phosphorous Content in the Sherds

A multilinear, regression model (MLR) including the Sr/Rb ratio and the absorbances at 980 cm^{-1} (maximum absorbance peak of albite), 1146 cm^{-1} (most probably K-feldspar), and 1515 cm^{-1} (aromatic OM), nicely fits the observed P concentrations (R = 0.92, MSE 0.16, RMSE 0.41; Figure 8).

We calculated the weights of these predictors on G-Cp2 for each sherd to determine the contribution of these compounds (OM and minerals). The weights of OM-P bearing compounds are positive in Guidoiro Areoso and Os Escurros; the weight of the Sr/Rb ratio is the dominant contributor for samples of A Lagoa and Requeán, while albite and K-feldspar control P content in Fraga do Zorro. These last two contributors show general positive contributions in the sherds from archaeological sites from areas dominated by felsic geological materials, although it is more obvious for the K-feldspar than for the albite. The low P contents in sherds from A Devesa, As Mamelas, and Devesa do Rei are due to the low contents of both P-bearing minerals (albite and K-feldspar) and organic (aromatic OM) compounds. It is also interesting to note that the variability in source contribution in the sherds from A Lagoa, a site characterized by domestic activity in disaggregated small spaces, is probably reflecting different small communities.

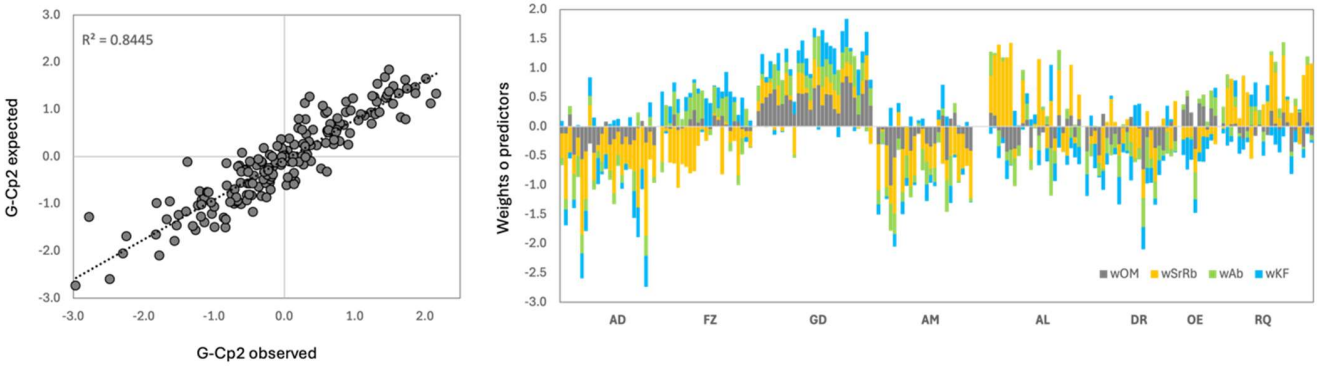

Figure 8. Left, scatterplot of observed and expected G-Cp2 scores. Right, distribution of weights of the four contributors (wOM: organic compounds; wAb: albite; wSrRb: Sr/Rb ratio; wKF: K-feldspar) to the G-Cp2 modeled by multilinear regression. Sites: AD: A devesa de Abaixo; FZ: Fraga do Zorro; GD: Guidoiro Areoso; AM: AS Mamelas; AL: A Lagoa; DR: Devesa do Rei; OE: Os Escurros; RQ: Requeán.

3.6. Archaeological Implications

The phosphorous content in the studied ceramics seems to mainly pertain two different sources: an inorganic source related to P-bearing minerals (albite and K-feldspar) and an organic (OM-P) source related to phosphorylated aromatic compounds. As already indicated, albite and K-feldspar are major P hosts in granitic rocks [42,63], and we may expect a larger contribution to P content in sherds from archaeological sites from felsic (i.e., granitic) areas. This is somewhat shown by the relatively higher contribution of K-feldspar in sherds from felsic areas, as suggested by the weights of the MLR model. But this is not fully systematical, as low contributions (i.e., negative weights) are found in sherds from A Devesa de Abaixo and As Mamelas, sites from the felsic areas, while high contributions (i.e., positive weights) are found in some sherds of Devesa do Rei and Requeán (Figure 8), which are sites from the mafic areas. Although a compositional effect due to the lithological background of the sites may be expected, as indicated by the chemical association of G-Cp1, temper minerals can result from intentional mixtures made by the ceramists, thus deviating the mineral composition of the sherds from the local dominant sources of the raw material.

The OM-P-bearing compounds, on the other hand, may have formed during firing by combustion of the organic matter contained in the raw material or plant remains intentionally added as temper, as previously suggested [66]. Lignin, a poly-aromatic biopolymer present in almost all plants and soil organic matter, has been shown to bind P due to its content of hydroxyl groups, forming very stable P-lignin compounds which are particularly resistant to thermal degradation at high temperature—lowering the combustibility of lignin when phosphorylated and making it more resistant to oxidation [67]. These properties are responsible for the use of phosphorylated lignin coatings as flame retardants [68–70] or for corrosion protection [71], for example. The phosphorylated aromatic OM of the sherds may have been selectively preserved due to its resistance to temperature (i.e., survive firing and cooking use) and to post-depositional microbial attack due to its resistance to oxidation processes. The addition of wood ashes, as found in ADE ceramics [40], can also be a source of phosphorylated OM, as phosphorus compounds are abundant in biochar [72]. On the other hand, low P contents are related to the presence of higher total OM contents, with a predominance of nitrogenated and aliphatic compounds, and kaolinite. This also lends support to our hypothesis, since lower P concentrations are related to sherds subjected to lower temperatures (or shorter firing time); kaolinite collapses at 550 °C, and higher aliphatic OM and total OM content were found in the inner sections of the sherds [66], where temperature may have been lower.

Our results also suggest that the P content in the sherds studied is related to the manufacturing of pottery. More specifically, inorganic P could be related to the selection

of raw materials and, therefore, the P content in the selected clays and inorganic temper. On the other hand, OM-P could be related to the elaboration of the pottery paste and the inclusion of plant OM as temper, which was burnt out during firing. The use of vessels as cooking pots could be another explanation for the presence of OM-P. It is known that enrichment in phosphorus can be a consequence of using pots for cooking [24,40]. However, the correlation of P with aromatic compounds instead of aliphatic compounds, normally understood as proxies of cooking activity [73,74], supports the idea that P enrichment in the studied sherds is due to the burnt organic temper, probably plants, manure, or soil organic matter [75–79]. Another possibility is the addition of bone fragments as temper, but hydroxyapatite was not detected in the FTIR-ATR spectra [80].

Considering that handmade pottery is a type of domestic activity related to close groups living together (i.e., families) that reproduce production recipes across generations [81–84], it can be hypothesized that the P content was influenced by these recipes. Our results did not show a relation between P and possible factors of diagenetic change (depositional context of pots) or cultural changes/differences between samples (chronology of the pots—Figures S2 and S3). On the contrary, sherds from settlements that are potential areas of production of handmade pottery show similarities in phosphorus content and between the inorganic sources of phosphorus (i.e., albite or albite and K-feldspar together). The only exception is the A Lagoa site, where the domestic activity was conducted in disaggregated small spaces that were probably from different small communities. The results obtained for this specific site reinforces the idea that different communities might have different production recipes for manufacturing pottery and for selecting raw materials, and these communities could be either all the inhabitants of a settlement or smaller or larger groups of people.

On the other hand, ceremonial and funerary sites, as Guidoiro Areoso, with similar P content in their samples could have been areas monopolized by one community, which was making pots with the same or similar recipes and bringing these vessels to their ceremonial sites. Another hypothesis is that the pottery from Guidoiro Areoso was made to be used on the site, including a specific recipe of raw materials for making the ceramic paste. The second hypothesis seems more likely due to the extreme regularity of P contents and P sources in Guidoiro Areoso from the Middle Neolithic to the Late Bronze Age. Therefore, Guidoiro Areoso might be a ritual center that had its own distinct pottery production, as some others have highlighted in the literature [85,86].

4. Conclusions

Our results have three general implications for the study of phosphorus in ancient pottery. First, we could not find evidence of phosphorus being significantly controlled by diagenetic processes or cooking activities. The absence of detectable secondary mineral phosphates and the negative correlation between P and aliphatic compounds may indicate different P sources than those traditionally noted in the literature.

Second, the evidence points to P content being a consequence of intentional and non-intentional actions in the pottery production process. Inorganic and organic sources of phosphorus were detected in the sherds. Organic phosphorus might be related to binding of the element to aromatic compounds, most likely during firing. Given the process of pottery manufacturing, we can assume that this association of phosphorus and OM resulted from the addition of organic temper to the pottery paste, likely as plant material, but also soil OM may have been present in the clays. The origin of inorganic phosphorus is related to the type of raw materials selected for molding the pots and the selection of the inorganic temper. Specifically, the relationship of phosphorus with albite and K-feldspar supports this idea.

And third, building on the last idea, our study shows that the combination of phosphorus studies and geochemical and mineralogical characterization of vessels reveals different recipes for pottery manufacturing (selection of raw materials and preparation of the pottery paste). These recipes seem to be specific to the sites where the ceramics were found,

indicating that pottery centers of production could be related either to a single settlement or to different communities inhabiting one specific area considered as a whole settlement (i.e., A Lagoa). Conversely, ceremonial and funerary sites might have been monopolized by one or several nearby communities that shared a similar recipe of making pottery at least regarding the use of P-bearing compounds (organic and inorganic). An alternative hypothesis could be that some ceremonial/funerary sites had an associated pottery production center, but this idea is only consistent with vessels from Guidoiro Areoso due to their extremely compositional homogeneity.

Supplementary Materials: The following supporting information can be downloaded at https://www.mdpi.com/article/10.3390/min14090880/s1, Section S1—Detailed information about pottery samples. This section provides detailed information about the sites where pottery samples were found, including the local lithology. It also includes information of the depositional context and chronology of each sample. Additionally, graphic materials related to the pottery and sites are provided. Section S2: Results: Supplementary Information. This section includes supporting tables and figures related to the results of this paper. Table S1. Mineralogical composition of the analyzed samples. Table S2. Average (avg) and standard deviation (std) of the concentrations (mg kg^{-1}) of the chemical elements determined by XRF in the studied sherds. Table S3. Loadings of the chemical elements determined by XRF in the studied sherds Figure S1. Correlation spectra for (a) G-Cp1 (background lithology) and (b) G-Cp3 (organic matter content). Figure S2: Cp2 in each site considering chronology of samples. Figure S3: Cp2 in each site considering context of deposition of samples.

Author Contributions: Conceptualization, A.M.C. and M.G.C.G.; methodology, A.M.C.; formal analysis, A.M.C.; investigation, A.M.C., M.G.C.G. and M.P.P.M.; resources, M.P.P.M.; data curation, A.M.C.; writing—original draft preparation, A.M.C. and M.G.C.G.; writing—review and editing, A.M.C. and M.G.C.G.; visualization, A.M.C. and M.G.C.G.; supervision, A.M.C.; project administration, M.P.P.M.; funding acquisition, M.P.P.M. and A.M.C. All authors have read and agreed to the published version of the manuscript.

Funding: This research was funded by MPPM (2007–2018) different projects. Two Research Projects from Xunta de Galicia ('Application of archaeometric techniques for the study of ancient Galician ceramics'—PGIDIT07PXIB236075PR, 2007-PG203, and 'Pb and Sr isotopes in archaeological ceramics from Galicia: study of provenance and access to raw materials'—EM 2012/054, 2012-PG217), and two Research Projects from the Spanish Ministry of Science and Innovation ('Ceramic styles in the Prehistory of Galicia: technology, raw materials and circulation'—HAR2010–17637, 2010-PN253, and 'Study of social change in the III and II millennia BC in the NW from the Iberian Peninsula from deposits of mixed context'—HAR2012−34029). EcoPast Research Group supported the analysis of Guidoiro Areoso samples (Grupos de Referencia Competitiva—ED431C 2021/32). M.G.C.G. was funded by a Xunta de Galicia Predoctoral Grant for Consolidación 2021 GRC GI-1553—EcoPast.

Data Availability Statement: Almost all data in provided in supporting material, but specific data will be available upon request to the authors.

Acknowledgments: We would like to thank the RIAIDT XRD and XRF facilities of the Universidade de Santiago de Compostela for the analytical support and the semiquantification of the mineral abundances. O. Lantes Suarez, technician of the RIAIDT, is also thanked for helping with preparation and analysis of some of the samples.

Conflicts of Interest: The authors declare no conflicts of interest.

References

1. Bintliff, J.; Degryse, P. A Review of Soil Geochemistry in Archaeology. *J. Archaeol. Sci. Rep.* **2022**, *43*, 103419. [CrossRef]
2. Wilson, C.A.; Davidson, D.A.; Cresser, M.S. Multi-Element Soil Analysis: An Assessment of Its Potential as an Aid to Archaeological Interpretation. *J. Archaeol. Sci.* **2008**, *35*, 412–424. [CrossRef]
3. Holliday, V.T.; Gartner, W.G. Methods of Soil P Analysis in Archaeology. *J. Archaeol. Sci.* **2007**, *34*, 301–333. [CrossRef]
4. Oonk, S.; Slomp, C.P.; Huisman, D.J. Geochemistry as an Aid in Archaeological Prospection and Site Interpretation: Current Issues and Research Directions. *Archaeol. Prospect.* **2009**, *16*, 35–51. [CrossRef]
5. Terry, R.E.; Nelson, S.D.; Carr, J.; Parnell, J.; Hardin, P.J.; Jackson, M.W.; Houston, S.D. Quantitative Phosphorus Measurement: A Field Test Procedure for Archaeological Site Analysis at Piedras Negras, Guatemala. *Geoarchaeology* **2000**, *15*, 151–166. [CrossRef]

6. King, S.M. The Spatial Organization of Food Sharing in Early Postclassic Households: An Application of Soil Chemistry in Ancient Oaxaca, Mexico. *J. Archaeol. Sci.* **2008**, *35*, 1224–1239. [CrossRef]
7. Fernández, F.G.; Terry, R.E.; Inomata, T.; Eberl, M. An Ethnoarchaeological Study of Chemical Residues in the Floors and Soils of Q'eqchi' Maya Houses at Las Pozas, Guatemala. *Geoarchaeol. Int. J.* **2002**, *17*, 487–519. [CrossRef]
8. García-López, Z.; Martínez Cortizas, A.; Álvarez-Fernández, N.; López-Costas, O. Understanding Necrosol Pedogenetical Processes in Post-Roman Burials Developed on Dunes Sands. *Sci. Rep.* **2022**, *12*, 10619. [CrossRef]
9. Farswan, Y.S.; Nautiyal, V. Investigation of Phosphorus Enrichment in the Burial Soil of Kumaun, Mid-Central Himalaya, India. *J. Archaeol. Sci.* **1997**, *24*, 251–258. [CrossRef]
10. Tallón Armada, R.; López Costas, O.; Martínez Cortizas, A. Análisis Del Contenido En Fósforo En Los Suelos y Sedimentos Del Yacimiento de Ventosiños (Coeses) Como Una Alternativa Al Hallazgo de Restos Óseos. In *Un Yacimiento Ceremonial en la Transición del Bronce al Hierro: Ventosiños (Coeses, Lugo)*; Cano Pan, J.A., Piay Augusto, D., Naveiro López, J., Eds.; Arqueoloxia do Noroeste SLU: Cambre, Spain, 2015; pp. 121–127.
11. Nielsen, N.H.; Kristiansen, S.M. Identifying Ancient Manuring: Traditional Phosphate vs. Multi-Element Analysis of Archaeological Soil. *J. Archaeol. Sci.* **2014**, *42*, 390–398. [CrossRef]
12. Horák, J.; Janovský, M.P.; Klír, T.; Malina, O.; Ferenczi, L. Multivariate Analysis Reveals Spatial Variability of Soil Geochemical Signals in the Area of a Medieval Manorial Farm. *Catena* **2023**, *220*, 106726. [CrossRef]
13. Devos, Y. Near Total and Inorganic Phosphorus Concentrations as a Proxy for Identifying Ancient Activities in Urban Contexts: The Example of Dark Earth in Brussels, Belgium. *Geoarchaeology* **2018**, *33*, 470–485. [CrossRef]
14. Lehmann, J.; Vabose Campos, C.; Luiz Casconselos de Mâncedo, H.; German, L. *Sequential P Fractionation of Relict Anthopogenic Dark Earths of Amazonia*; Glaser, B., Woods, W., Eds.; Springer: Berlin/Heidelberg, Germany, 2004; ISBN 9783662056837.
15. Wilson, L.; Pollard, A.M. Here Today, Gone Tomorrow? Integrated Experimentation and Geochemical Modeling in Studies of Archaeological Diagenetic Change. *Acc. Chem. Res.* **2002**, *35*, 644–651. [CrossRef] [PubMed]
16. Neff, D.; Dillmann, P.; Bellot-Gurlet, L.; Beranger, G. Corrosion of Iron Archaeological Artefacts in Soil: Characterisation of the Corrosion System. *Corros. Sci.* **2005**, *47*, 515–535. [CrossRef]
17. Nord, A. On the Deterioration of Archaeological Iron Artefacts in Soil. *Fornvännen* **2002**, *97*, 298–300.
18. Hedges, R.E.M. Bone Diagenesis: An Overview of Processes. *Archaeometry* **2002**, *44*, 319–328. [CrossRef]
19. Kendall, C.; Eriksen, A.M.H.; Kontopoulos, I.; Collins, M.J.; Turner-Walker, G. Diagenesis of Archaeological Bone and Tooth. *Palaeogeogr. Palaeoclimatol. Palaeoecol.* **2018**, *491*, 21–37. [CrossRef]
20. López-Costas, O.; Lantes-Suárez, Ó.; Martínez Cortizas, A. Chemical Compositional Changes in Archaeological Human Bones Due to Diagenesis: Type of Bone vs Soil Environment. *J. Archaeol. Sci.* **2016**, *67*, 43–51. [CrossRef]
21. Maggetti, M. Phase Analysis and Its Significance for Technology and Origin. In *Archaeological Ceramics*; Olin, J.S., Franklin, A.D., Eds.; Smithsonian Institution Press: Washington, DC, USA, 1982; pp. 121–133.
22. Rice, P.M. Recent Ceramic Analysis: 1. Function, Style, and Origins. *J. Archaeol. Res.* **1996**, *4*, 133–163. [CrossRef]
23. Rice, P.M. Recent Ceramic Analysis: 2. Composition, Production, and Theory. *J. Archaeol. Res.* **1996**, *4*, 165–202. [CrossRef]
24. Maritan, L. Archaeo-Ceramic 2.0: Investigating Ancient Ceramics Using Modern Technological Approaches. *Archaeol. Anthropol. Sci.* **2019**, *11*, 5085–5093. [CrossRef]
25. Maggetti, M.; Heinmann, R.B. Experiments on Simulated Burial of Calcareous Terra Sigillata (mineralogical change). Preliminary Results. *Br. Museum Occas. Pap.* **1981**, *19*, 163–177.
26. Maritan, L. Ceramic Abandonment. How to Recognise Post-Depositional Transformations. *Archaeol. Anthropol. Sci.* **2020**, *12*, 199. [CrossRef]
27. Schwedt, A.; Mommsen, H.; Zacharias, N.; Buxeda i Garrigós, J. Analcime Crystallization and Compositional Profiles—Comparing Approaches to Detect Post-Depositional Alterations in Archaeological Pottery. *Archaeometry* **2006**, *48*, 237–251. [CrossRef]
28. Stoner, W.D.; Shaulis, B.J. Chemical Mapping to Evaluate Post-Depositional Diagenesis among the Earliest Ceramics in the Teotihuacan Valley, Mexico. *Minerals* **2021**, *11*, 384. [CrossRef]
29. Gilstrap, W.D.; Meanwell, J.L.; Paris, E.H.; López Bravo, R.; Day, P.M. Post-depositional Alteration of Calcium Carbonate Phases in Archaeological Ceramics: Depletion and Redistribution Effects. *Minerals* **2021**, *11*, 749. [CrossRef]
30. Maritan, L.; Angelini, I.; Artioli, G.; Mazzoli, C.; Saracino, M. Secondary Phosphates in the Ceramic Materials from Frattesina (Rovigo, North-Eastern Italy). *J. Cult. Herit.* **2009**, *10*, 144–151. [CrossRef]
31. Golitko, M.; McGrath, A.; Kreiter, A.; Lightcap, I.V.; Duffy, P.R.; Parditka, G.M.; Giblin, J.I. Down to the Crust: Chemical and Mineralogical Analysis of Ceramic Surface Encrustations on Bronze Age Ceramics from Békés 103, Eastern Hungary. *Minerals* **2021**, *11*, 436. [CrossRef]
32. Aoyama, H.; Yamagiwa, K.; Fujimoto, S.; Izumi, J.; Ganeko, S.; Kameshima, S. Non-Destructive Elemental Analysis of Prehistoric Potsherds in the Southern Ryukyu Islands, Japan: Consideration of the Pottery Surface Processing Technique in the Boundary Region between the Japanese Jōmon and Neolithic Taiwan. *J. Archaeol. Sci. Reports* **2020**, *33*, 102512. [CrossRef]
33. Gosselain, O.P. *Poteries Du Cameroun Méridional: Styles Techniques et Rapports à L'identité*; CNRS ÉDITIONS: Paris, France, 2002; ISBN 2-271-06034-6.
34. Colas, C. Présence de Céramiques à Dégraissant Osseux Dans Les Régions de l'ouest de La France. *Bull. Société Préhistorique Française* **1996**, *93*, 534–542. [CrossRef]

35. Kowalski, Ł.; Weckwerth, P.; Chabowski, M.; Adamczak, K.; Jodłowski, P.; Szczepańska, G.; Chajduk, E.; Polkowska-Motrenko, H.; Kozicka, M.; Kukawka, S. Towards Ritualisation: Insights into Bone-Tempered Pottery from the TRB Settlement in Kałdus (Poland, 3500–3350 BC). *Ceram. Int.* **2020**, *46*, 3099–3112. [CrossRef]
36. Odriozola, C.P.; Hurtado Pérez, V.M. The Manufacturing Process of 3rd Millennium BC Bone Based Incrusted Pottery Decoration from the Middle Guadiana River Basin (Badajoz, Spain). *J. Archaeol. Sci.* **2007**, *34*, 1794–1803. [CrossRef]
37. Díaz-del-Río, P.; Consuegra, S.; Domínguez, R.; Martín-Bañón, A.; Vírseda, L.; Agua, F.; Villegas, M.Á.; García-Heras, M. Identificación de Una Tradición Tecnológica Cerámica Con Desgrasante Óseo En El Neolítico Peninsular. Estudio Arqueométrico de Materiales Cerámicos de Madrid (5300-3400 Cal AC). *Trab. Prehist.* **2011**, *68*, 99–122. [CrossRef]
38. Opriș, V.; Velea, A.; Secu, M.; Rostas, A.M.; Buruiană, A.T.; Simion, C.A.; Mirea, D.A.; Matei, E.; Bartha, C.; Dimache, M.; et al. 'Put Variety in White': Multi-Analytical Investigation of the White Pigments Inlaid on Early Chalcolithic Pottery from Southern Romania. *J. Archaeol. Sci. Rep.* **2022**, *42*, 103402. [CrossRef]
39. Gomart, L.; Burnez-Lanotte, L. Technique de Façonnage, Production Céramique et Identité de Potiers: Une Approche Technologique de La Céramique de Style Non Rubané Du Site Du Staberg à Rosmeer (Limbourg, Belgique). *Bull. Société Préhistorique Française* **2012**, *109*, 231–250. [CrossRef]
40. Rodrigues, S.F.S.; da Costa, M.L. Phosphorus in Archeological Ceramics as Evidence of the Use of Pots for Cooking Food. *Appl. Clay Sci.* **2016**, *123*, 224–231. [CrossRef]
41. Perišić, N.; Marić-Stojanović, M.; Andrić, V.; MIOč, U.B.; Damjanović, L. Physicochemical Characterisation of Pottery from the Vinča Culture, Serbia, Regarding the Firing Temperature and Decoration Techniques. *J. Serbian Chem. Soc.* **2016**, *81*, 1415–1426. [CrossRef]
42. London, D.; Cerny, P.; Loomis, J.L.; Pan, J.J. Phosphorus in Alkali Feldspars of Rare-Element Granitic Pegmatites. *Can. Mineral.* **1990**, *28*, 771–786.
43. Chung, F.H. Quantitative Interpretation of X-Ray Diffraction Patterns of Mixtures. I. Matrix-Flushing Method for Quantitative Multicomponent Analysis. *J. Appl. Crystallogr.* **1974**, *7*, 519–525. [CrossRef]
44. Lantes Suárez, Ó.; Prieto Martínez, M.P.; Martínez Cortizas, A. Caracterización de Pastas Blancas Incrustadas En Decoraciones de Campaniformes Gallegos. In *dagando Sobre Su Procedencia. In VIII Congreso Ibérico de Arqueometría*; Saíz Carrasco, M.E., López Romero, R., Cano Díaz-Tendero, M.A., Calvo García, J.C., Eds.; Seminario de Arqueología y Etnología Turolense; SAET: Teruel, Spain, 2009; pp. 87–99.
45. Martínez Cortizas, A.; Lantes Suárez, Ó.; Prieto Martínez, M.P. Análisis Arqueométrico de La Cerámica de Contextos Campaniforme Del Área Ulla-Deza. In *Reconstruyendo la Historia de la Comarca del Ulla-Deza (Galicia, España). Escenarios Arqueológicos del Pasado. TAPA 41*; Prieto Martínez, M.P., Criado Boado, F., Eds.; Consejo Superior de Investigaciones Científicas. Laboratorio de Arqueoloxía do Insituto de Estudos Padre Sarmiento; Xunta de Galicia: Santaigo de Compostela, Spain, 2010; pp. 135–145, ISBN 9781119130536.
46. Prieto Martínez, M.P.; Martínez Cortizas, A.; Lantes Suárez, Ó.; Guimarey, B. Cerámicas Campaniformes de Galicia (NW de España): Caracterización Arqueométrica y Estudio de La Procedencia de Algunos Yacimientos Representativos. *Cuad. Prehist. Arqueol.* **2015**, *41*, 109–125. [CrossRef]
47. Salanova, L.; Prieto Martínez, M.P.; Clop García, X.; Convertini, F.; Lantes Suárez, Ó.; Martínez Cortizas, A. What Are Large-Scale Archaeometric Programmes for? Bell Beaker Pottery and Societies from the Third Millennium BC in Western Europe. *Archaeometry* **2016**, *58*, 722–735. [CrossRef]
48. Demšar, J.; Curk, T.; Erjavec, A.; Gorup, Č.; Hočevar, T.; Milutinovič, M.; Možina, M.; Polajnar, M.; Toplak, M.; Starič, A.; et al. Orange: Data Mining Toolbox in Python. *J. Mach. Learn. Res.* **2013**, *14*, 2349–2353.
49. Bollong, C.A.; Vogel, J.C.; Jacobson, L.; van der Westhuizen, W.A.; Sampson, C.G. Direct Dating and Identity of Fibre Temper in Pre-Contact Bushman (Basarwa) Pottery. *J. Archaeol. Sci.* **1993**, *20*, 41–55. [CrossRef]
50. Ionescu, C.; Hoeck, V.; Ghergari, L. Electron Microprobe Analysis of Ancient Ceramics: A Case Study from Romania. *Appl. Clay Sci.* **2011**, *53*, 466–475. [CrossRef]
51. Duma, G. Phosphate Content of Ancient Pots as Inidcation of Use. *Curr. Anthropol.* **1972**, *13*, 127–130. [CrossRef]
52. da Costa, M.L.; Kern, D.C.; Pinto, A.H.E.; Souza, J.R.D.T. The Ceramic Artifacts in Archaeological Black Earth (terra preta) from Lower Amazon Region, Brazil: Chemistry and Geochemical Evolution. *Acta Amaz.* **2004**, *34*, 375–386. [CrossRef]
53. Costa, M.L.; Rios, G.M.; da Silva, M.M.C.; da Silva, G.J.; Molano-Valdes, U. Mineralogia e Química de Fragmentos Cerâmicos Arqueológicos Em Sítio Com Terra Preta Da Amazônia Colombiana. *Rev. Esc. Minas* **2011**, *64*, 17–23. [CrossRef]
54. Legodi, M.A.; de Waal, D. Raman Spectroscopic Study of Ancient South African Domestic Clay Pottery. *Spectrochim. Acta Part Mol. Biomol. Spectrosc.* **2007**, *66*, 135–142. [CrossRef] [PubMed]
55. Iordanidis, A.; Garcia-Guinea, J.; Karamitrou-Mentessidi, G. Analytical Study of Ancient Pottery from the Archaeological Site of Aiani, Northern Greece. *Mater. Charact.* **2009**, *60*, 292–302. [CrossRef]
56. Belfiore, C.M.; Di Bella, M.; Triscari, M.; Viccaro, M. Production Technology and Provenance Study of Archaeological Ceramics from Relevant Sites in the Alcantara River Valley (North-Eastern Sicily, Italy). *Mater. Charact.* **2010**, *61*, 440–451. [CrossRef]
57. Freestone, I.C.; Meeks, N.D.; Middleton, A.P. Retention of Phosphate in Buried Ceramics: An Electron Microbieam Approarch. *Archaeometry* **1985**, *27*, 161–177. [CrossRef]
58. Fabbri, B.; Gualtieri, S. Reasons of Phosphorus Pollution in Archaeological Pottery and Its Consequences: A Reassessment. In *New Developments in Archaeology Research*; Adalslteinn, M., Olander, T., Eds.; Nov. Sci. Publ.: New York, NY, USA, 2013; pp. 41–66.

59. Costa, M.L.; Rodrigues, S.F.S.; Silva, G.J.S.; Pöllmann, H. Crandallite Formation in Archaeological Potteries Found in the Amazonian Dark Earth Soils. In Proceedings of the 10th International Congress for Applied Mineralogy (ICAM), Trondheim, Norway, 2–5 August 2011; Maarten, A.T.M.B., Ed.; Springer: Trondheim, Norway, 2012; pp. 137–138.
60. Gasparini, E.; Tarantino, S.C.; Ghigna, P.; Riccardi, M.P.; Cedillo-González, E.I.; Siligardi, C.; Zema, M. Thermal Dehydroxylation of Kaolinite under Isothermal Conditions. *Appl. Clay Sci.* **2013**, *80–81*, 417–425. [CrossRef]
61. Berzina-Cimdina, L.; Borodajenko, N. Research of Calcium Phosphates Using Fourier Transform Infrared Spectroscopy. In *Infrared Spectroscopy—Materials Science, Engineering and Technology*; Theopanides, T., Ed.; IntechOpen: London, UK, 2012; pp. 123–148.
62. Brangule, A.; Gross, K.A. Importance of FTIR Spectra Deconvolution for the Analysis of Amorphous Calcium Phosphates. In *IOP Conference Series: Materials Science and Engineering*; IOP Publishing: Bristol, UK, 2015; Volume 77. [CrossRef]
63. Breiter, K.; Frýda, J.; Leichmann, J. Phosphorus and Rubidium in Alkali Feldspars: Case Studies and Possible Genetic Interpretation. *Bull. Czech Geol. Surv.* **2002**, *77*, 93–104.
64. Prieto Martínez, M.P.; Lantes Suárez, Ó.; Martínez Cortizas, A.M. Dos Enterramientos de La Edad Del Bronce de La Provincia de Ourense. *Rev. Aquae Flaviae* **2009**, *41*, 93–105.
65. Rajan, S.S.S. Changes in Net Surface Charge of Hydrous Alumina with Phosphate Adsorption. *Nature* **1976**, *262*, 45–46. [CrossRef]
66. Kaal, J.; Lantes Suárez, Ó.; Martínez Cortizas, A.M.; Prieto Lamas, B.; Prieto Martínez, M.P.; Lantes-Suárez, O.; Martínez Cortizas, A.M.; Prieto, B.; Prieto Martínez, M.P. How Useful Is Pyrolysis-GC/MS for the Assessment of Molecular Properties of Organic Matter in Archaeological Pottery Matrix? An Exploratory Case Study from North-West Spain. *Archaeometry* **2014**, *56*, 187–207. [CrossRef]
67. Prieur, B.; Meub, M.; Wittemann, M.; Klein, R.; Bellayer, S.; Fontaine, G.; Bourbigot, S. Phosphorylation of Lignin: Characterization and Investigation of the Thermal Decomposition. *RSC Adv.* **2017**, *7*, 16866–16877. [CrossRef]
68. Ferry, L.; Dorez, G.; Taguet, A.; Otazaghine, B.; Lopez-Cuesta, J.M. Chemical Modification of Lignin by Phosphorus Molecules to Improve the Fire Behavior of Polybutylene Succinate. *Polym. Degrad. Stab.* **2015**, *113*, 135–143. [CrossRef]
69. Guo, Y.; Cheng, C.; Huo, T.; Ren, Y.; Liu, X. Highly Effective Flame Retardant Lignin/Polyacrylonitrile Composite Prepared via Solution Blending and Phosphorylation. *Polym. Degrad. Stab.* **2020**, *181*, 109362. [CrossRef]
70. Zhang, S.; Li, S.N.; Wu, Q.; Li, Q.; Huang, J.; Li, W.; Zhang, W.; Wang, S. Phosphorus Containing Group and Lignin toward Intrinsically Flame Retardant Cellulose Nanofibril-Based Film with Enhanced Mechanical Properties. *Compos. Part B Eng.* **2021**, *212*, 108699. [CrossRef]
71. Chaudhari, T.; Rajagopalan, N.; Dam-Johansen, K. Lignin Phosphate: A Biobased Substitute for Zinc Phosphate in Corrosion-Inhibiting Coatings. *ACS Sustain. Chem. Eng.* **2024**, *12*, 7813–7830. [CrossRef]
72. Bekiaris, G.; Peltre, C.; Jensen, L.S.; Bruun, S. Using FTIR-Photoacoustic Spectroscopy for Phosphorus Speciation Analysis of Biochars. *Spectrochim. Acta Part A Mol. Biomol. Spectrosc.* **2016**, *168*, 29–36. [CrossRef]
73. Heimann, R.B. Ancient and Historical Cooking Pots and Food: An Eternal Communion. A Topical Review. *Archaeometry* **2024**, 1–16. [CrossRef]
74. Copley, M.S.; Berstan, R.; Dudd, S.N.; Aillaud, S.; Mukherjee, A.J.; Straker, V.; Payne, S.; Evershed, R.P. Processing of Milk Products in Pottery Vessels through British Prehistory. *Antiquity* **2005**, *79*, 895–908. [CrossRef]
75. Kulkova, M.; Kulkov, A. The Identification of Organic Temper in Neolithic Pottery from Russia and Belarus. *Old Potter's Alm.* **2016**, *21*, 2–12.
76. Dzhanfezova, T. 'Organic Temper' and the Early Neolithic Pottery Production: Interpretational Challenges. *Acta Archaeol.* **2020**, *91*, 61–87. [CrossRef]
77. Casanova, E.; Knowles, T.D.J.; Bayliss, A.; Dunne, J.; Barański, M.Z.; Denaire, A.; Lefranc, P.; di Lernia, S.; Roffet-Salque, M.; Smyth, J.; et al. Accurate Compound-Specific 14C Dating of Archaeological Pottery Vessels. *Nature* **2020**, *580*, 506–510. [CrossRef] [PubMed]
78. Gabasio, M.; Evin, J.; Arnal, G.B.; Andrieux, P. Origins of Carbon in Potsherds. *Radiocarbon* **1986**, *28*, 711–718. [CrossRef]
79. Livingstone Smith, A. *Chaîne Opératoire de La Poterie. Références Ethnographiques, Analyses et Reconstitution*; Musée Royal de l'Afrique Centrale: Tervuren, Belgium, 2007; ISBN 9789074752237.
80. Mamede, A.P.; Vassalo, A.R.; Piga, G.; Cunha, E.; Parker, S.F.; Marques, M.P.M.; Batista De Carvalho, L.A.E.; Gonçalves, D. Potential of Bioapatite Hydroxyls for Research on Archeological Burned Bone. *Anal. Chem.* **2018**, *90*, 11556–11563. [CrossRef]
81. Bowser, B.J.; Patton, J.Q. Learning and Transmission of Pottery Style: Women's Life Histories and Communities of Practice in the Ecuadorian Amazon. In *Cultural Transmission and Material Culture: Breaking Down Boundaries*; Stark, M.T., Bowser, B.J., Horne, L., Eds.; The University of Arizona Press: Tucson, AZ, USA, 2008; pp. 105–129.
82. Cámara Manzaneda, J.; García Rosselló, J.; López-Cachero, F.J.; Clop García, X. Ceramic Production and Household Organisation of Late Bronze Age Communities: Forming Processes and Spatial Distribution of the Ceramic Vessels of Genó (North-Eastern Iberian Peninsula). *Trab. Prehist.* **2022**, *79*, 67–84. [CrossRef]
83. Wallaert-Pêtre, H. Learning How to Make the Right Pots: Apprenticeship Strategies and Material Culture, a Case Study in Handmade Pottery from Cameroon. *J. Anthropol. Res.* **2001**, *57*, 471–493. [CrossRef]
84. Gosselain, O.; Livingstone Smith, A. The Source. Clay Selection and Processing Practices in Sub-Saharan Africa. In *Breaking the Mould: Challenging the Past through Pottery*; Berg, I., Ed.; BAR International Series; Archaeopress: Oxford, UK, 2005; pp. 33–47, ISBN 1841716952.

85. Thompson, V.D.; Stoner, W.D.; Rowe, H.D. Early Hunter-Gatherer Pottery along the Atlantic Coast of the Southeastern United States: A Ceramic Compositional Study. *J. Isl. Coast. Archaeol.* **2008**, *3*, 191–213. [CrossRef]
86. Šegvić, B.; Šešelj, L.; Slovenec, D.; Lugović, B.; Ferreiro Mählmann, R. Composition, Technology of Manufacture, and Circulation of Hellenistic Pottery from the Eastern Adriatic: A Case Study of Three Archaeological Sites along the Dalmatian Coast, Croatia. *Geoarchaeology* **2012**, *27*, 63–87. [CrossRef]